Relating cloud condensation nuclei activity and oxidation level of α-pinene secondary organic aerosols

M. Frosch,[1] M. Bilde,[1] P. F. DeCarlo,[2,3] Z. Jurányi,[2,4] T. Tritscher,[2] J. Dommen,[2] N. M. Donahue,[5] M. Gysel,[2] E. Weingartner,[2] and U. Baltensperger[2]

Received 15 June 2011; revised 5 September 2011; accepted 13 September 2011; published 30 November 2011.

[1] During a series of smog chamber experiments, the effects of chemical and photochemical aging on the ability of organic aerosols generated from ozonolysis of α-pinene to act as cloud condensation nuclei (CCN) were investigated. In particular, the study focused on the relation between oxygenation and the CCN-derived single hygroscopicity parameter κ for different experimental conditions: varying precursor concentrations (10–40 ppb), different OH sources (photolysis of HONO either with or without the addition of NO or ozonolysis of tetramethylethylene), and exposure to light. Oxygenation was described by the contribution of the aerosol mass spectrometer (AMS) mass fragment m/z 44 to the total organic signal (f_{44}) and the oxygen to carbon molar ratio (O/C), likewise determined with AMS. CCN activity, described by the hygroscopicity parameter κ, was determined with a CCN counter. It was found that f_{44} increases with decreasing precursor concentration and with chemical aging, whereas neither of these affects CCN activity. Overall, κ is largely independent of O/C in the range $0.3 < \mathrm{O/C} < 0.6$ ($0.07 < f_{44} < 0.12$), although an empirical unweighted least squares fit was determined: $\kappa = (0.071 \pm 0.02) \cdot (\mathrm{O/C}) + (0.0785 \pm 0.009)$ for particles with diameter in the range 59–200 nm. Growth kinetics of activating secondary organic aerosols were found to be comparable to those of ammonium sulfate and were not influenced by chemical aging.

Citation: Frosch, M., M. Bilde, P. F. DeCarlo, Z. Jurányi, T. Tritscher, J. Dommen, N. M. Donahue, M. Gysel, E. Weingartner, and U. Baltensperger (2011), Relating cloud condensation nuclei activity and oxidation level of α-pinene secondary organic aerosols, *J. Geophys. Res.*, *116*, D22212, doi:10.1029/2011JD016401.

1. Introduction

[2] Atmospheric aerosol particles can affect global climate either by direct interaction with solar radiation or by the so-called indirect effect, where particles take up water and grow into cloud droplets [*Intergovernmental Panel on Climate Change*, 2007]. Radiative properties of clouds depend on the size and number concentration of droplets, which is governed by atmospheric conditions, such as the number of cloud condensation nuclei (CCN) and the supersaturation of water. The ability of aerosol particles to act as CCN depends on the particle size and chemical composition. Atmospheric aerosols often comprise a complex, internal mixture, of which organic compounds constitutes a major fraction [e.g., *Hallquist et al.*, 2009; *Jimenez et al.*, 2009]. The organic fraction also contributes to the CCN activity of the aerosol particles. Some organic matter is introduced to the atmosphere through primary emissions, and some is formed as secondary organic aerosols (SOA) through condensation of products from gas phase oxidation of volatile organic compounds (VOC) of either biogenic or anthropogenic origin. Several studies have been carried out on the CCN activity of SOA, either sampled directly from the atmosphere [e.g., *McFiggans et al.*, 2005; *Chang et al.*, 2010; *Roberts et al.*, 2010]; or from smog chamber experiments [e.g., *Duplissy et al.*, 2008; *Jurányi et al.*, 2009; *George and Abbatt*, 2010; *Poulain et al.*, 2010; *Lambe et al.*, 2011a, 2011b]. Among the most important biogenic SOA precursors are monoterpenes, such as α-pinene [*Kanakidou et al.*, 2005].

[3] *Duplissy et al.* [2008] investigated SOA from photooxidation of α-pinene and found that water uptake in the subsaturated regime (at RH = 95%) strongly depends on precursor concentration, with precursor concentration ranging from 10 to 183 ppb. Both hygroscopicity and the degree of oxygenation depend on chemical age [e.g., *McFiggans et al.*, 2005]. *Poulain et al.* [2010] concluded that hygroscopicity as well as volatility is related to the degree of oxygenation, likewise under subsaturated conditions (RH =

[1]Department of Chemistry, University of Copenhagen, Copenhagen, Denmark.
[2]Laboratory of Atmospheric Chemistry, Paul Scherrer Institut, Villigen, Switzerland.
[3]Now at Department of Civil, Architectural, and Environmental Engineering, Drexel University, Philadelphia, Pennsylvania, USA.
[4]Now at School of Engineering, Institute of Aerosol and Sensor Technology, University of Applied Sciences Northwestern Switzerland, Windisch, Switzerland.
[5]Center for Atmospheric Particle Studies, Carnegie Mellon University, Pittsburgh, Pennsylvania, USA.

0148-0227/11/2011JD016401

99%), in agreement with recent findings [*Duplissy et al.*, 2011; *Tritscher et al.*, 2011]. A relation between hygroscopicity at subsaturated conditions and the degree of oxygenation has also been observed for ambient aerosols [e.g., *Jimenez et al.*, 2009]. Several studies have compared hygroscopic properties at RH < 100% to CCN activation. For example, both *Duplissy et al.* [2008] and *Jurányi et al.* [2009] reported correspondence within experimental uncertainties between hygroscopicity determined under sub- and supersaturated conditions for SOA produced from photooxidation of α-pinene (with initial precursor concentration of 10–270 ppb). In contrast, *Prenni et al.* [2007] observed discrepancies for SOA produced from ozonolysis of α-pinene, although the initial precursor concentration was much greater (>400 ppb) than in the studies by *Duplissy et al.* [2008] and *Jurányi et al.* [2009].

[4] *Jurányi et al.* [2009] also investigated the dependence of the CCN activity on precursor concentration (in the range 10–270 ppb) for SOA from α-pinene, and while that study confirms the relation between precursor concentration and hygroscopicity for RH < 100% as shown by *Duplissy et al.* [2008], a similar trend is not observed for the CCN activity within experimental uncertainty. Furthermore, no variation of CCN activity as a function of chemical aging was detected. The relation between CCN activity of organic aerosol particles and the oxygen to carbon molar ratio (O/C) has been studied in field campaigns and chamber studies, but no clear trend has been discerned [*Chang et al.*, 2010; *Massoli et al.*, 2010; *Roberts et al.*, 2010; *Lambe et al.*, 2011b]. However, previous studies have demonstrated that properties such as molar mass and density can also significantly influence CCN activity [*Petters et al.*, 2009a] for compounds with similar functional groups, almost identical elemental composition and thereby also very similar O/C [*Rosenørn et al.*, 2006].

[5] In contrast to these results, *Engelhart et al.* [2008] studied CCN activity for SOA produced from ozonolysis of α-pinene, either with or without an OH scavenger, and observed an increase in CCN activity over time in experiments without an OH scavenger, at least for the first few hours after the initial reaction. For experiments where SOA was generated in the presence of an OH scavenger, no statistically significant trend in CCN activity was observed. At the end of each experiment (after ~9 h), SOA had approximately the same CCN activity in the two types of experiments.

[6] *Engelhart et al.* [2008] produced SOA at a substantially lower relative humidity (RH = 3%–8%) than *Jurányi et al.* [2009] (RH = 50%–60%) and the physical properties of SOA have been shown to depend on the amount of water vapor available [*Poulain et al.*, 2010]. Finally, *Duplissy et al.* [2008] found that monodisperse SOA particles generated photochemically from α-pinene in the presence of NO_x (at RH = 53%) became increasingly more CCN active after 3–23 h of illumination.

[7] In this work, we study the effect of chemical aging on the CCN activity of SOA produced from ozonolysis of α-pinene and aged with OH under various conditions. We investigate the relation between the single hygroscopicity parameter κ derived from CCN activation and oxygenation for a range of smog chamber experiments with varying precursor concentration, various OH sources and duration of OH exposure.

2. Theory

[8] The equilibrium saturation ratio of water (S) for an aqueous solution droplet with known size and chemical composition can be determined using the Köhler equation [*Köhler*, 1936]. Here we express it in the following way [*Seinfeld and Pandis*, 1998; *Kreidenweis et al.*, 2005]:

$$S = \frac{p}{p_0} = a_w \cdot \exp\left(\frac{4M_w\sigma_{al}}{RT\rho_w D_p}\right), \quad (1)$$

where a_w is the water activity, M_w is the molar weight of water, σ_{al} is the air-liquid surface tension, R is the ideal gas constant, T is the absolute temperature, ρ_w is the density of water, and D_p is the droplet diameter. From the saturation ratio, the supersaturation, SS = $(S-1)\cdot 100\%$ is determined. A plot of SS versus D_p is called a Köhler curve, and the maximum defines the so-called critical supersaturation, SS_c.

[9] The relationship between the water content of the droplet and water activity can be described by the single hygroscopicity parameter κ, introduced by *Petters and Kreidenweis* [2007]:

$$\frac{1}{a_w} = 1 + \kappa\frac{V_s}{V_w}, \quad (2)$$

where V_s is the solute volume (dry particle volume) and V_w is the water volume. The most hygroscopic species found in ambient aerosols have a maximum κ of ~1.3, whereas κ = 0 means that the particle is insoluble in water. Combining equations (1) and (2) yields the equation defining the "κ-Köhler theory" [*Petters and Kreidenweis*, 2007]:

$$\mathrm{SS} = \left(\frac{D_p^3 - D_{\mathrm{dry}}^3}{D_p^3 - D_{\mathrm{dry}}^3(1-\kappa)}\exp\left(\frac{4M_w\sigma_{al}}{RT\rho_w D_p}\right) - 1\right)\cdot 100\%, \quad (3)$$

where D_{dry} is the diameter of the dry particle. If κ for a particle with diameter D_{dry} is inserted into equation (3), the maximum of SS as a function of D_p is equal to the critical supersaturation.

3. Experimental Procedure

3.1. SOA Formation and Aging

[10] SOA formation from α-pinene and ageing were carried out at Paul Scherrer Institut (PSI) during the Multiple Chamber Aerosol Chemistry and Aging Study (MUCHACHAS) campaign in a 27 m^3 Teflon reaction chamber. The general procedure in the MUCHACHAS experiments was to generate SOA from ozonolysis of α-pinene without addition of an OH scavenger, allow SOA to stabilize and then expose it to OH radicals to observe changes caused by OH aging. The smog chamber at PSI has been described in detail by *Paulsen et al.* [2005], and the smog chamber operation during the MUCHACHAS campaign has been described by *Tritscher et al.* [2011], but will be briefly outlined in the following.

[11] A summary of all experiments is given in Table 1. The temperature in the smog chamber was approximately

Table 1. Summary of Smog Chamber Experiments

Experiment	Date	α-Pinene Conc.,[b] ppb	Ozone		SC Lights		OH Source[a] (HONO/TME)		Dry Size (CCN) Diameter, nm	Comments
			Time,[c] h	Conc., ppb	ON[c]	OFF[c]	ON[c]	OFF[c]		
No Additional OH Source										
a	6 Feb	10	0	200	3.25	5.3	–	–	100	
					7.25	9.3				
b	14 Jan	40	0	200	4.8	7.0	–	–	–	No CCN data
c	26 Jan	40	0	500	–	–	–	–	125	
d	18 Feb	40	0	500	–	–	–	–	133	No AMS data
Dark OH Source (TME)										
e	9 Feb	10	0	500	4.5	6.5	1.9	–	75–100	
			1.5	150	8.5	10.6				
f	2 Feb	10	0	500	21.3	–	2.6	–	100	
			2.4	150			5.8			
			7.4	150						
g	28 Jan	40	0	500	–	–	1.6	24.7	–	No CCN data
			1.5	200						
h	23 Feb	10	0	500	–	–	3.2	9.8	59	No AMS data
i	25 Feb	10	0	500	5.9	8.5	1.6	6.3	59	No AMS data
Light OH Source (HONO), High NO_x										
j[d]	23 Jan	10	0	200	4.7	9.7	4.7	9.4	75–125	
k[e]	13 Feb	40	0	150	4.7	8.9	4.7	8.9	95–113	
			1.2	100						
l[f]	19 Jan	40	0	90	5.2	10.3	5.2	10.3	75–200	
			3.0	20						
Light OH Source (HONO), Low NO_x										
m	11 Feb	10	0	250	2.7	4.7	2.7	4.7	75–100	
			1.9	50	6.8	9.3	6.8	9.2		
n	21 Jan	10	0	150	4.6	8.9	4.6	8.3	100–125	
			0.5	50						

[a]HONO was photolysed to produce OH (injection of HONO started ~1 h before lights were turned on); TME reacted with ozone to produce OH.
[b]Nominal concentration determined from the volume of injected α-pinene, assuming a smog chamber volume of 27 m^3.
[c]Time is hours after injection of α-pinene.
[d]At 4.5 h after α-pinene injection: [NO] = 60 ppb.
[e]At 4.3 h after α-pinene injection: [NO] = 80 ppb.
[f]At 5.1 h after α-pinene injection: [NO] = 50 ppb.

20°C. The chamber was humidified to a relative humidity of 50%–60% before introducing first 150–500 ppb ozone and then α-pinene. The relative humidity level is comparable to previous studies [e.g., *Duplissy et al.*, 2008; *Jurányi et al.*, 2009]. In some experiments, extra amounts of ozone were added to ensure that oxidation of the full amount of precursor occurred fast, before particulate material was lost to the smog chamber walls.

[12] A known amount of α-pinene (either 1.8 or 7.2 μl) was evaporated by heating it to 80°C in a glass sampling bulb and flushing it into the chamber with purified air, resulting in a nominal concentration of α-pinene in the smog chamber of either 10 or 40 ppb, calculated from the volume of injected α-pinene, assuming a smog chamber volume of 27 m^3. No seed aerosol was used in any of the experiments. The first section of each experiment consisted of the preparation of SOA from ozonolysis of α-pinene. During the second part of the experiments an OH source was added, instigating condensation and aging mediated by OH. In one type of experiments an OH source was not added (experiments a–d in Table 1). Two OH sources were used; either ozonolysis of tetramethylethylene (TME, systematic name: 2,3-dimethyl-2-butene; experiments e–i in Table 1) in the dark or photolysis of HONO, either with or without the addition of NO (experiments j–l and m–n in Table 1, respectively). Solar light was simulated with four xenon arc lamps (16 kW total). HONO was added continuously for approximately 1 h before the lights were turned on until lights were turned off. The injection system of HONO was designed according to *Taira and Kanda* [1990]; the level of HONO was measured by a Long Path Absorption Photometer (LOPAP) to be approximately 15–20 ppbv [*Heland et al.*, 2001]. Furthermore, during some experiments, the lights were occasionally cycled on and off (see Table 1) to evaluate the effect of light induced chemistry. TME was injected continuously from a gas cylinder (Messer, 1000 ppm (by moles) TME in N_2) at a flow rate of 10 ml/min. Ozone was present in excess prior to TME addition.

3.2. Instruments

[13] SOA was characterized with the Aerodyne high-resolution time-of-flight aerosol mass spectrometer (AMS) [*DeCarlo et al.*, 2006] and a continuous-flow streamwise thermal-gradient CCN counter (DMT CCNC-100) [*Roberts and Nenes*, 2005]. The CCNC was used to determine the size-dependent critical supersaturation of SOA. Particles leaving the smog chamber were dried in a diffusion drier containing Silica Gel and sent through a neutralizer and a differential mobility analyzer (DMA, custom built, equivalent to TSI, model 3071) which was operated with an aerosol

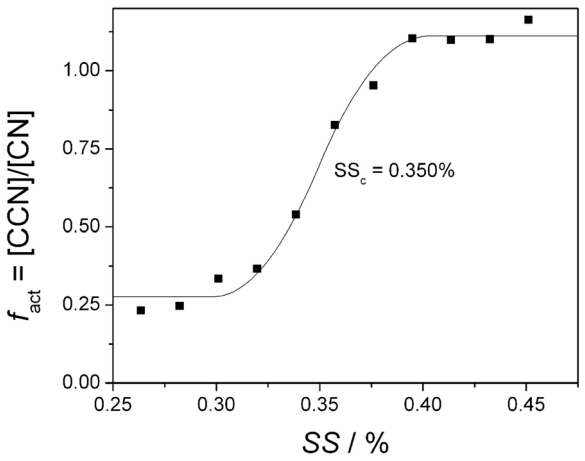

Figure 1. Example of the determination of SS_c (the supersaturation at which 50% of the singly charged particles are activated) of 100 nm secondary organic aerosol (SOA) particles produced in experiment e (see Table 1) approximately 7 h after α-pinene injection. Experimental data (individual points) are fitted to a relaxed step function (solid line). Multiply charged particles are responsible for $f_{act} > 0$ at low supersaturations, while for high supersaturations, $f_{act} > 1$ is due to experimental uncertainties.

to sheath flow ratio of either 1:10 or 1:16. The DMA selected a quasi-monodisperse sample flow with a known dry diameter (D_{dry}) which was then split between a condensation particle counter (CPC, TSI 3022A) and the CCNC. The CCNC was calibrated using dry ammonium sulfate particles; measurements for the calibration were obtained regularly, both before, during and after the series of smog chamber experiments. During both calibrations and measurements, the sheath flow of the CCNC was 0.450 l/min, and the sample flow was 0.045 l/min, resulting in a flow ratio of 1:10.

[14] During experiments, the supersaturation in the CCNC was varied stepwise between 0.05% and 2%, and the activated fraction f_{act}, i.e., the ratio between the total number concentration ([CN], measured with the CPC) and the number concentration of activated particles ([CCN], measured with the CCNC), was depicted as a function of SS. See Figure 1 for an example. SS_c was determined by correcting for doubly charged particles and fitting the data set to a relaxed step function [*Svenningsson and Bilde*, 2008]. To avoid a high level of doubly charged particles, the diameter of the monodisperse aerosol was mainly chosen to be above the mode of the size distribution in the smog chamber (diameter range 59–200 nm). The aerosol particle size distribution (with diameters in the range 20–800 nm) was measured with a scanning mobility particle sizer (SMPS). An SS_c measurement lasted approximately 20–30 min.

[15] For a given mass transfer coefficient of water vapor, activated CCN will grow to cloud droplets of similar diameter (D_{wet}) if exposed to the same supersaturation, not depending on chemical composition. The optical particle counter (OPC) of the CCNC measures droplet size and can therefore assess growth kinetics of activating particles. Some organic compounds can delay or even hinder water uptake and activation [*Nenes et al.*, 2001; *Asa-Awuku and Nenes*, 2007; *Asa-Awuku et al.*, 2009]. This effect was evaluated by comparing D_{wet} (determined by the OPC) of activated SOA to D_{wet} of activated ammonium sulfate particles (also determined from the OPC) at the same critical supersaturation (similar to the approach of, e.g., *Engelhart et al.* [2008] and *Asa-Awuku et al.* [2009, 2010]). Since the CCN activity of ammonium sulfate in general is different from the CCN activity of SOA, the dry diameter of ammonium sulfate particles activating at a given supersaturation is different than the dry diameter of SOA activating at the same supersaturation, but if CCN experiments are carried out under identical conditions of instrument operation the activated droplets will grow to the same size when detected by the OPC. This technique is called threshold droplet growth analysis (TDGA) [e.g., *Bougiatioti et al.*, 2009]. The aim was therefore not to report the actual size of the activated particles, but to detect any differences between activated SOA and ammonium sulfate particles. D_{wet} of activated ammonium sulfate particles were determined for supersaturations in the range 0.1%–0.9%, see Figure 2.

[16] The AMS measures the chemical composition of nonrefractory components of submicron aerosols and has been described in detail elsewhere [e.g., *DeCarlo et al.*, 2006; *Canagaratna et al.*, 2007]. Briefly, the AMS uses an aerodynamic lens to direct particles to a heated tungsten surface (~600°C) where the nonrefractory components are vaporized and ionized with electron ionization at 70 eV. A high-resolution time-of-flight mass spectrometer records the resulting mass spectrum. Data was processed in custom software (Squirrel 1.47, http://cires.colorado.edu/jimenez-group/ToFAMSResources/ToFSoftware/index.html). Oxygen to carbon molar ratios (O/C) were calculated on the high-resolution mass spectra from the methods described by *Aiken et al.* [2007, 2008], using only ion fragments generally associated with organic species. f_{44} was calculated from

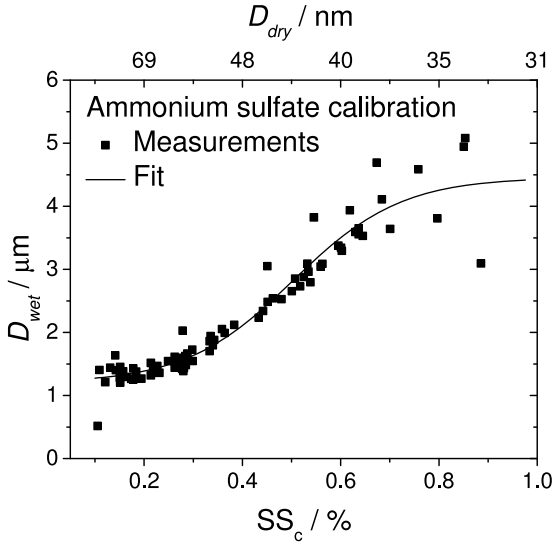

Figure 2. Droplet diameter of activated ammonium sulfate particles (D_{wet}) determined from the optical particle counter (OPC) as a function of SS_c or dry particle diameter (D_{dry}). The solid line is an empirical fit (sigmoidal function).

the unit mass resolution data as the mass ratio of *m*/*z* 44 to total organic signal excluding nominally inorganic fragments. On the basis of measurements for high mass concentration (before significant SOA amounts were lost to the chamber walls), the standard deviation of 1 h of measurement was approximately 0.0005 in experiments with a precursor concentration of 40 ppb (see Table 1) and 0.001 for experiments with a precursor concentration of 10 ppb (greater mass concentration and higher signal in the 40 ppb experiments are the reasons for the improved precision).

[17] Fourteen experiments were carried out in the smog chamber, and in nine of them both the AMS and the CCNC were successfully operated. In two experiments, no CCNC data were available (experiments b and g; see Table 1), and in three experiments no AMS data were available (experiments d, h, and i; see Table 1).

4. Results and Discussion

[18] Figure 3 shows κ and the contribution of the AMS mass fragment *m*/*z* 44 to the total organic signal (f_{44}) as a function of time for the four types of experiments performed. It is clear that a high precursor concentration (40 ppb, red lines/points) corresponds to a low f_{44}, as has been previously observed in several chamber studies [e.g., *Duplissy et al.*, 2008; *Shilling et al.*, 2009; *Massoli et al.*, 2010]. The value of f_{44} is 7%–12%, which is in the same range as reported in previous studies of photo-oxidation [*Duplissy et al.*, 2008] and ozonolysis of α-pinene [*George and Abbatt*, 2010; *Poulain et al.*, 2010; *Lambe et al.*, 2011a], and it increases slightly with time. We attribute this increase to condensation of higher oxidation state compounds generated from second generation chemistry and possibly also heterogeneous oxidation of SOA. However, the latter mechanism is expected to be significantly slower due to diffusion limitations [*Lambe et al.*, 2009]. No clear temporal trend beyond experimental uncertainties is observed for κ. This is consistent with the results of *Jurányi et al.* [2009]. Physical properties influencing κ include molecular weight, density, activity coefficient, surface tension and solubility of SOA. The effects of solubility and activity coefficient on κ are assumed to be negligible within the studied range of experimental conditions [e.g., *Petters et al.*, 2009b; *Lambe et al.*, 2011b], whereas fragmentation or oligomerization leading to formation of low- or high-molecular-weight species may have strong effect on κ, as may surface tension depression [e.g., *Petters et al.*, 2009a; *Lambe et al.*, 2011b]. However, the evolution of such properties during particle aging was evidently not strong enough to influence CCN derived κ.

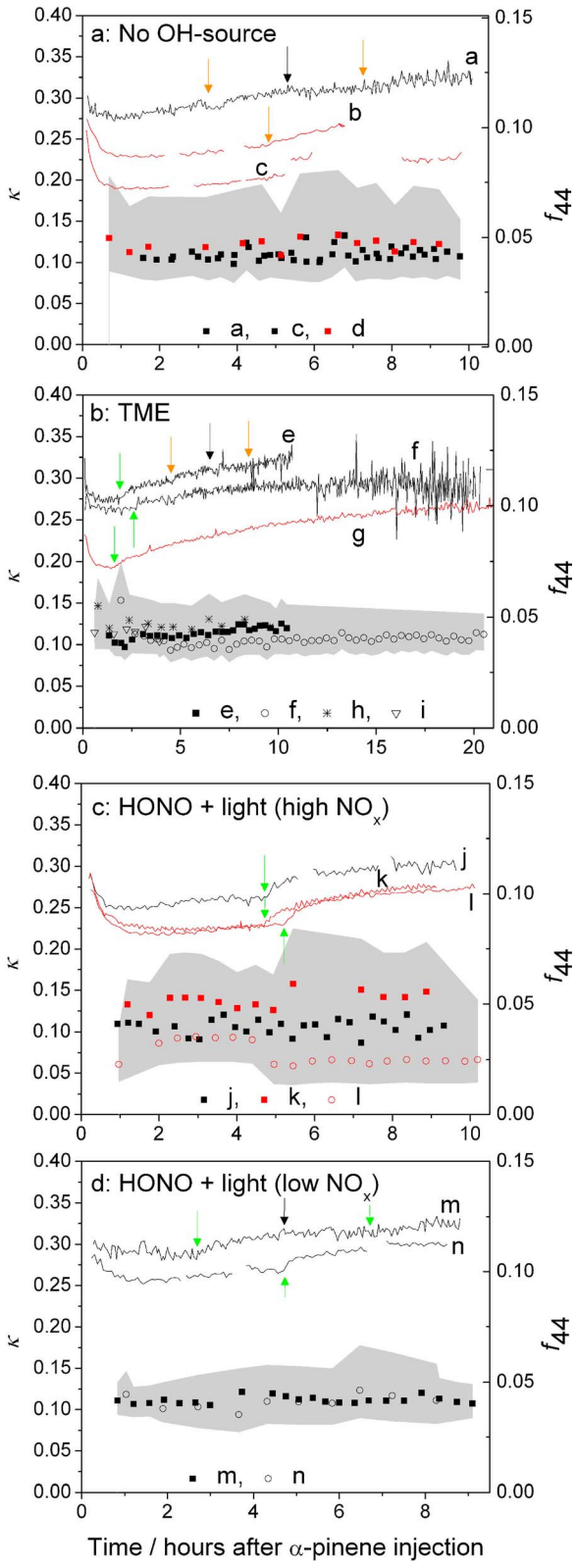

Figure 3. The contribution of the AMS mass fragment *m*/*z* 44 to the total organic signal, f_{44} (solid lines, right axis) and κ (symbols, left axis) with (a) periods of lights on but no additional OH source (experiments a–d), (b) ozonolysis of tetramethylethylene (TME) as OH source (experiments e–i), (c) photolysis of HONO as OH source with addition of NO (experiments j–l), and (d) photolysis of HONO as OH source (no addition of NO) (experiments m–n). All experiments start with ozonolysis of α-pinene. Arrows indicate when lights are turned on (orange arrows) and off (black arrows) and when an OH source is added (green arrows). Solid lines and symbols represent experiments with low precursor concentration (10 ppb) and red lines and symbols represent experiments with high precursor concentration (40 ppb). Estimated uncertainties in κ are shown as shading. Letters a–n refer to experiments listed in Table 1.

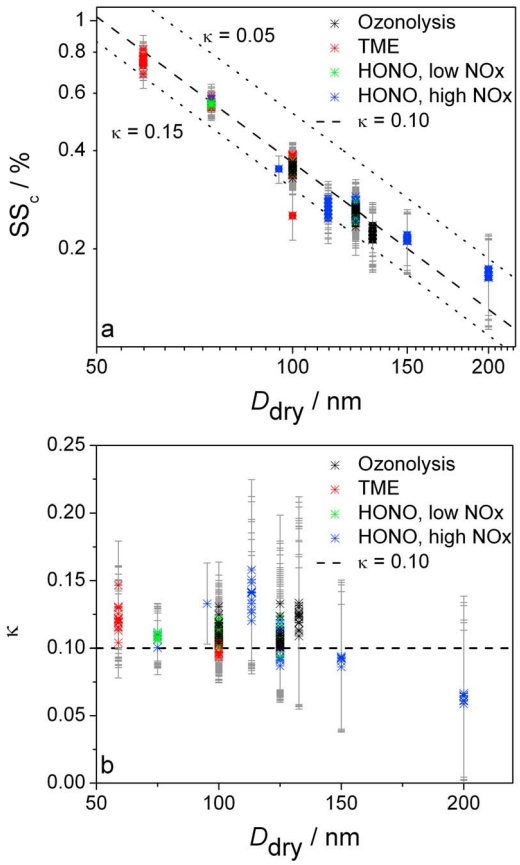

Figure 4. (a) Critical supersaturation and (b) single hygroscopicity parameter κ as a function of dry particle diameter (D_{dry}) for all cloud condensation nucleus (CCN) experiments during all smog chamber experiments. Uncertainties for each individual point are given by error bars.

[19] It should be noted that AMS data are integrated over all particle sizes, whereas κ is determined from monodisperse particle distributions. This may induce uncertainties, since the chemical composition may not be identical for all particle sizes. As the DMA coupled to the CCNC was set to select particles above the mode of the size distribution in the smog chamber, during most experiments the number of particles in the smog chamber with diameters greater than the one selected with the DMA was so small that their contribution to the total volume was <50% (data not shown). However, to the extent that the SOA is in equilibrium with semivolatile organic components, the chemical composition should be independent of particle size.

[20] As listed in Table 1, during several experiments lights were turned on. In experiments j–n, this was done to instigate photolysis of HONO (OH source). In the remaining experiments, lights were turned on and off to explore the differences between light and dark chemistry. This is indicated in Figure 3 by green, orange and black arrows. However, also in these cases, light leads to the formation of OH radicals by photolysis of ozone and photolysis of aldehydic products. In Figures 3a and 3b lights being on causes an increase in f_{44} but no change in κ. In Figures 3c and 3d a pronounced increase in f_{44} is seen, simultaneous with the lights being turned on (except the second "light on" in experiment m), which initiates condensation of newly formed products from OH reactions. *Tritscher et al.* [2011] distinguishes between four phases during each smog chamber experiment: First, formation of SOA during the first 1–2 h followed by aging (termed "ripening"), which is proceeded by condensation and ripening by the addition of an OH source. The growth factor derived κ values were found to increase during condensation and remain constant during ripening. This was observed for both the ozonolysis and the OH reaction regimes. As seen in Figure 4, the addition of HONO and light, NO_x or TME does not appear to influence the CCN derived hygroscopicity parameter κ beyond experimental uncertainties. Figure 4a compares the critical supersaturation as a function of dry particle diameter (D_{dry}) for all CCN experiments to a line of constant κ (0.10). Figure 4b shows κ as a function of D_{dry}. Since Figure 3 shows no significant dependency of κ on precursor concentration or OH exposure, an average $\kappa = 0.11 \pm 0.02$ is determined. This is consistent with other studies of SOA produced from α-pinene in smog chambers [e.g., *Prenni et al.*, 2007; *Duplissy et al.*, 2008; *Jurányi et al.*, 2009; *George and Abbatt*, 2010] and with the growth factor derived κ for SOA produced in the PSI smog chamber during the MUCHACHAS campaign, which has recently been reported by *Tritscher et al.* [2011].

[21] However, κ is not constant for all D_{dry} but slightly smaller (down to approximately 0.06) for the largest diameters. This may be related to the fact that in general κ is slightly dependent on water activity [*Petters and Kreidenweis*, 2007; *Petters et al.*, 2009b], and that water activity at activation depends on D_{dry}.

[22] Furthermore, the uncertainty of κ was greater for the largest particles (see Figure 4b). This is because these activated at very low critical supersaturation, close to the limit of the supersaturation range of the CCNC. A slight decrease in growth factor derived κ with increasing dry particle size (with diameters in the range 50–150 nm) was also reported

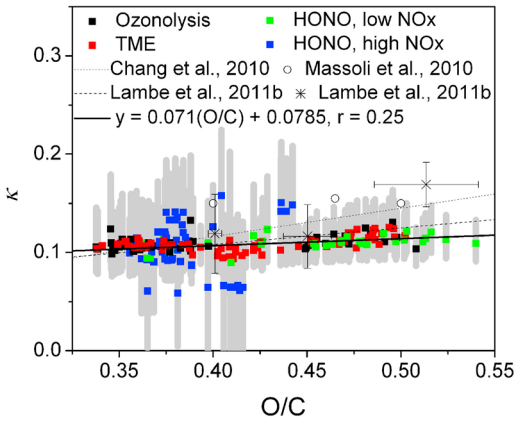

Figure 5. Hygroscopicity parameter κ for particles with dry diameter in the range 59–200 nm as a function of the oxygen to carbon molar ratio (O/C). Uncertainties are shown as shading. An unweighted least squares fit and coefficient of linear correlation [*Taylor*, 1997] are shown and compared to the correlations and data points reported by *Chang et al.* [2010], *Massoli et al.* [2010], and *Lambe et al.* [2011b].

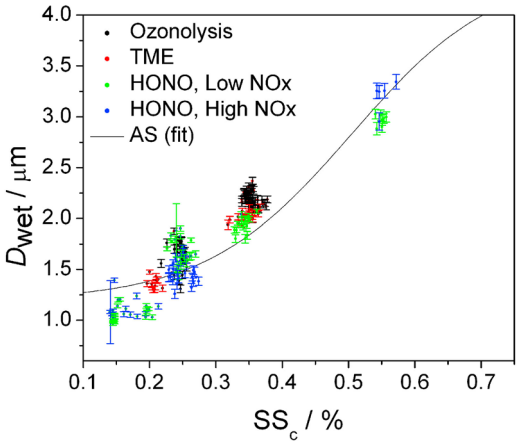

Figure 6. Droplet diameter of activated particles (D_{wet}) determined from the OPC as a function of critical supersaturation for SOA particles with diameters in the range 59–200 nm. The individual points from smog chamber experiments are compared to the average droplet size obtained from ammonium sulfate (AS) calibrations (valid in the supersaturation range 0.1% to 0.9%; see Figure 2).

by *Tritscher et al.* [2011], although the variation did not exceed experimental uncertainty.

[23] Figure 5 shows κ as a function of the oxygen to carbon molar ratio, O/C. All κ values for particles with diameters between 59 and 200 nm are included in Figure 5. Considering the experimental uncertainties, it is not possible to establish a clear connection between O/C and κ. Nevertheless, an unweighted least squares linear fit results in $\kappa = (0.071 \pm 0.02) \cdot (O/C) + (0.0785 \pm 0.009)$ for 59 nm $< D_{dry} <$ 200 nm and 0.3 < O/C < 0.6. All data obtained from the present study are well fit by a straight line, regardless of the presence and type of OH source, and the dependence of κ on O/C is weak (Figure 5).

[24] *Chang et al.* [2010] also determined an empirical correlation between O/C and κ for the organic component of ambient aerosols, $\kappa_{org} = (0.29 \pm 0.05) \cdot (O/C)$ for 0.3 < O/C < 0.6 ($0.07 < f_{44} < 0.12$); shown in Figure 5. This parameterization has a steeper slope resulting in higher κ for O/C > 0.36. The overall κ value of 0.15 for the entire organic fraction, reported by *Chang et al.* [2010], is also greater than the measured κ values depicted in Figure 5, and even greater is κ of the oxygenated organic fraction, which *Chang et al.* [2010] reports as 0.22 ± 0.04 (determined by assuming the unoxygenated organic fraction is nonhygroscopic). However, the study by Chang et al. focused on particles sampled from ambient air, which may account for the deviation from SOA generated from ozonolysis/photochemistry of α-pinene.

[25] *Lambe et al.* [2011b] found a relation between O/C and κ of SOA generated from oxidation of a variety of precursors under exposure to OH and determined the following relation: $\kappa_{org} = (0.17 \pm 0.04) \cdot (O/C) + 0.04$, which is also shown in Figure 5 together with the measured κ for SOA from oxidation of α-pinene. Although the parameterization is based on the properties of SOA generated from many different precursors, it agrees well with the data obtained from ozonolysis of α-pinene in the present study, as does the data points for O/C < 0.5 reported by *Lambe et al.* [2011b].

[26] A recent chamber study [*Massoli et al.*, 2010] indicates that the relation between CCN derived κ and O/C for SOA generated from oxidation of 40–80 ppb α-pinene with an OH exposure of up to 10^{12} molecules · cm^{-3} · s is nonuniform. In particular, the dependency between O/C and κ value is strongest at high O/C (O/C > 0.75), whereas the response of κ to changes of O/C is rather insignificant at O/C < ~0.5. Furthermore, *Massoli et al.* [2010] conclude that κ at a certain O/C also depends on the precursor experimental conditions, such as OH exposure. For comparison, the data points obtained by *Massoli et al.* [2010] for α-pinene SOA in the range 0.3 < O/C < 0.55 are shown in Figure 5. These κ values are also largely independent of O/C in this range of O/C values, but higher than the κ values observed in the present study. *Massoli et al.* [2010] generated SOA from OH oxidation in the absence of NO_x. The observed difference in κ at comparable O/C could partially be caused by difference in chemistry, due to this experimental procedure. Weak sensitivity of CCN derived κ to O/C is observed in the range 0.3 < O/C < 0.6 consistent with *Massoli et al.* [2010] and in contrast to the sensitivity of HTDMA derived κ to O/C [*Duplissy et al.*, 2011; *Tritscher et al.*, 2011]. The discrepancy between water uptake at subsaturated conditions and CCN activity has previously been examined, and has been linked to nonideal interactions at low water activities [*Petters et al.*, 2009b]. However, although CCN derived κ versus O/C has a rather flat plateau in the studied range ($0.3 < \kappa < 0.6$), κ depends more strongly on O/C beyond this range. For example, at very low O/C κ is minimal, which is related to low solubility, whereas a steep relationship was observed for O/C > 0.75, probably due to fragmentation after high OH exposure resulting in the production of species with low molar weight [*Massoli et al.*, 2010; *Lambe et al.*, 2011b].

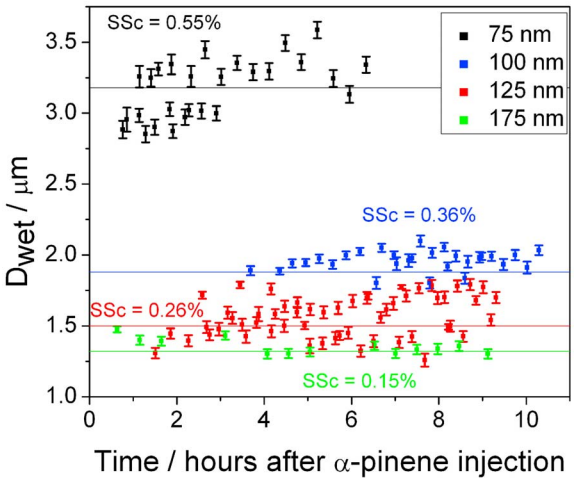

Figure 7. Diameter of activated SOA particles (symbols) as a function of time for four different dry particle sizes compared to the diameter of activated ammonium sulfate particles with the same critical supersaturation, assuming $\kappa_{SOA} = 0.11$ (horizontal lines).

[27] *Kuwata et al.* [2011] evaluated the effect of thermodenuder treatment on CCN activity as a function of O/C in the range ~0.4 < O/C < ~0.5 for SOA generated from ozonolysis of α-pinene. Particles exposed to a low temperature in the thermodenuder (25°C) did not exhibit any correlation between κ and O/C within the studied range. However, for particles exposed to high temperatures (up to 100°C) in the thermodenuder, κ depended strongly on both temperature and organic particle mass concentration, M_{org}. The interpretation of this behavior was that evaporation of high-volatility species in the thermodenuder was accompanied by oligomerization, increasing the fraction of low-volatility oligomers. The high effective molar mass of the produced oligomers significantly decreased CCN activity. This effect was deemed more important at low M_{org}, because SOA under these conditions contained a mix of functional groups (aldehydes and ketones), more favorable to oligomerization.

[28] The effect of organics on the growth kinetics of the activating SOA particles is explored in Figure 6, where D_{wet}, the wet diameter of the activated particles measured by the OPC, is plotted as a function of SS_c, both for ammonium sulfate particles (black line) and for SOA (individual points). The droplet diameter of activated SOA does not differ significantly from that of ammonium sulfate. This is in agreement with the findings of *Engelhart et al.* [2008]. Figure 7 shows D_{wet} as a function of time after the start of ozonolysis of α-pinene for four different dry particle diameters (individual points). For comparison the D_{wet} of ammonium sulfate particles after activation at the same SS_c (assuming $\kappa_{SOA} = 0.11$) is also shown (horizontal lines). No trend beyond experimental uncertainty is observed.

5. Conclusions

[29] The CCN derived κ of SOA, generated from ozonolysis of α-pinene and aged under a variety of experimental conditions, has been determined and compared to O/C and to f_{44}, derived from AMS measurements. f_{44} decreases with increasing precursor concentration and increases with chemical aging, but κ (derived from CCN activation experiments) does not depend either on the oxidative process, e.g., precursor concentration, the presence of an OH source or NO_x, or type and extent of chemical aging for the investigated experimental conditions. κ derived from CCN activation experiments is largely independent of O/C in the range of 0.3 < O/C < 0.6 (0.07 < f_{44} < 0.12), although a slight increase in κ as a function of O/C is indicated by an empirical least squares fit. However, the experimental uncertainties are too great to establish a relationship between the two parameters. This is in contrast to a clear dependence of hygroscopic growth factors at RH < 100% on O/C, which has previously been reported in literature. Growth kinetics of the activating SOA particles are comparable to ammonium sulfate and are not hindered by SOA or influenced by chemical aging.

[30] **Acknowledgments.** We acknowledge the financial support by the EC project EUROCHAMP, the IMBALANCE project of the Competence Center for Environment and Sustainability, and the Swiss National Science Foundation and the Villum Kann Rasmussen Foundation. P.F.D. is grateful for postdoctoral research support from the U.S. NSF (IRFP 0701013).

References

Aiken, A. C., P. F. DeCarlo, and J. L. Jimenez (2007), Elemental analysis of organic species with electron ionization high-resolution mass spectrometry, *Anal. Chem.*, *79*, 8350–8358, doi:10.1021/ac071150w.

Aiken, A. C., et al. (2008), O/C and OM/OC ratios of primary, secondary, and ambient organic aerosols with high-resolution time-of-flight aerosol mass spectrometry, *Environ. Sci. Technol.*, *12*, 4478–4485, doi:10.1021/es703009q.

Asa-Awuku, A., and A. Nenes (2007), Effect of solute dissolution kinetics on cloud droplet formation: Extended Köhler theory, *J. Geophys. Res.*, *112*, D22201, doi:10.1029/2005JD006934.

Asa-Awuku, A., G. J. Engelhart, B. H. Lee, S. N. Pandis, and A. Nenes (2009), Relating CCN activity, volatility, and droplet growth kinetics of β-caryophyllene secondary organic aerosol, *Atmos. Chem. Phys.*, *9*, 795–812, doi:10.5194/acp-9-795-2009.

Asa-Awuku, A., A. Nenes, S. Gao, R. C. Flagan, and J. H. Seinfeld (2010), Water-soluble SOA from alkene ozonolysis: Composition and droplet activation kinetics inferences from analysis of CCN activity, *Atmos. Chem. Phys.*, *10*, 1585–1597, doi:10.5194/acp-10-1585-2010.

Bougiatioti, A., C. Fountoukis, N. Kalivitis, S. N. Pandis, A. Nenes, and N. Mihalopoulos (2009), Cloud condensation nuclei measurements in the marine boundary layer of the eastern Mediterranean: CCN closure and droplet growth kinetics, *Atmos. Chem. Phys.*, *9*, 7053–7066, doi:10.5194/acp-9-7053-2009.

Canagaratna, M. R., et al. (2007), Chemical and microphysical characterization of ambient aerosols with the aerodyne aerosol mass spectrometer, *Mass Spectrom. Rev.*, *26*, 185–222, doi:10.1002/mas.20115.

Chang, R. Y.-W., J. G. Slowik, N. C. Shantz, A. Vlasenko, J. Liggio, S. J. Sjostedt, W. R. Leaitch, and J. P. D. Abbatt (2010), The hygroscopicity parameter (κ) of ambient organic aerosol at a field site subject to biogenic and anthropogenic influences: Relationship to degree of aerosol oxidation, *Atmos. Chem. Phys.*, *10*, 5047–5064, doi:10.5194/acp-10-5047-2010.

DeCarlo, P. F., et al. (2006), Field-deployable high-resolution time-of-flight aerosol mass spectrometer, *Anal. Chem.*, *78*, 8281–8289, doi:10.1021/ac061249n S0003-2700(06)01249-2.

Duplissy, J., et al. (2008), Cloud forming potential of secondary organic aerosol under near atmospheric conditions, *Geophys. Res. Lett.*, *35*, L03818, doi:10.1029/2007GL031075.

Duplissy, J., et al. (2011), Relating hygroscopicity and composition of organic aerosol particulate matter, *Atmos. Chem. Phys.*, *11*, 1155–1165, doi:10.5194/acp-11-1155-2011.

Engelhart, G. J., A. Asa-Awuku, A. Nenes, and S. N. Pandis (2008), CCN activity and droplet growth kinetics of fresh and aged monoterpene secondary organic aerosol, *Atmos. Chem. Phys.*, *8*, 3937–3949, doi:10.5194/acp-8-3937-2008.

George, I. J., and J. P. D. Abbatt (2010), Chemical evolution of secondary organic aerosol from OH-initiated heterogeneous oxidation, *Atmos. Chem. Phys.*, *10*, 5551–5563, doi:10.5194/acp-10-5551-2010.

Hallquist, M., et al. (2009), The formation, properties and impact of secondary organic aerosol: Current and emerging issues, *Atmos. Chem. Phys.*, *9*, 5155–5236, doi:10.5194/acp-9-5155-2009.

Heland, J., J. Kleffmann, R. Kurtenbach, and P. Wiesen (2001), A new instrument to measure gaseous nitrous acid (HONO) in the atmosphere, *Environ. Sci. Technol.*, *35*, 3207–3212, doi:10.1021/es000303t.

Intergovernmental Panel on Climate Change (2007), *Climate Change 2007—The Physical Science Basis: Contribution of Working Group I to the Fourth Assessment Report of the IPCC*, Cambridge Univ. Press, Cambridge, U. K.

Jimenez, J. L., et al. (2009), Evolution of organic aerosols in the atmosphere, *Science*, *326*, 1525–1529, doi:10.1126/science.1180353.

Jurányi, Z., et al. (2009), Influence of gas-to-particle partitioning on the hygroscopic and droplet activation behaviour of α-pinene secondary organic aerosol, *Phys. Chem. Chem. Phys.*, *11*, 8091–8097, doi:10.1039/b904162a.

Kanakidou, M., et al. (2005), Organic aerosol and global climate modelling: A review, *Atmos. Chem. Phys.*, *5*, 1053–1123, doi:10.5194/acp-5-1053-2005.

Köhler, H. (1936), The nucleus in and the growth of hygroscopic droplets, *Trans. Faraday Soc.*, *32*, 1152–1161, doi:10.1039/tf9363201152.

Kreidenweis, S. M., K. Koehler, P. J. DeMott, A. J. Prenni, C. Carrico, and B. Ervens (2005), Water activity and activation diameters from hygroscopicity data—Part I. Theory and application to inorganic salts, *Atmos. Chem. Phys.*, *5*, 1357–1370, doi:10.5194/acp-5-1357-2005.

Kuwata, M., Q. Chen, and S. T. Martin (2011), Cloud condensation nuclei (CCN) activity and oxygen-to-carbon elemental ratios following thermodenuder treatment of organic particles grown by α-pinene ozonolysis, *Phys. Chem. Chem. Phys.*, *13*, 14,571–14,583, doi:10.1039/c1cp20253g.

Lambe, A. T., M. A. Miracolo, C. J. Hennigan, A. L. Robinson, and N. M. Donahue (2009), Effective rate constants and uptake coefficients for the reactions of organic molecular markers (*n*-alkanes, hopanes, and steranes) in motor oil and diesel primary organic aerosols with OH radicals, *Environ. Sci. Technol.*, *43*, 8794–8800, doi:10.1021/es901745h.

Lambe, A. T., T. B. Onasch, P. Massoli, D. R. Croasdale, J. P. Wright, A. T. Ahern, L. R. Williams, D. R. Worsnop, W. H. Brune, and P. Davidovits (2011a), Laboratory studies of the chemical composition and cloud condensation nuclei (CCN) activity of secondary organic aerosol (SOA) and oxidized primary organic aerosol (OPOA), *Atmos. Chem. Phys.*, *11*, 8913–8928, doi:10.5194/acp-11-8913-2011.

Lambe, A. T., et al. (2011b), Characterization of aerosol photooxidation flow reactors: Heterogeneous oxidation, secondary organic aerosol formation and cloud condensation nuclei activity measurements, *Atmos. Meas. Technol.*, *4*, 445–461, doi:10.5194/amt-4-445-2011.

Massoli, P., et al. (2010), Relationship between aerosol oxidation level and hygroscopic properties of laboratory generated secondary organic aerosol (SOA) particles, *Geophys. Res. Lett.*, *37*, L24801, doi:10.1029/2010GL045258.

McFiggans, G., et al. (2005), Simplification of the representation of the organic component of atmospheric particulates, *Faraday Discuss.*, *130*, 341–362, doi:10.1039/b419435g.

Nenes, A., S. Ghan, H. Abdul-Razzak, P. Y. Chuang, and J. H. Seinfeld (2001), Kinetic limitations on cloud droplet formation and impact on cloud albedo, *Tellus, Ser. B*, *53*, 133–149, doi:10.1034/j.1600-0889.2001.d01-12.x.

Paulsen, D., J. Dommen, M. Kalberer, A. S. H. Prevot, R. Richter, M. Sax, M. Steinbacher, E. Weingartner, and U. Baltensperger (2005), Secondary organic aerosol formation by irradiation of 1,3,5-trimethylbenzene-NO_x-H_2O in a new reaction chamber for atmospheric chemistry and physics, *Environ. Sci. Technol.*, *39*, 2668–2678, doi:10.1021/es0489137.

Petters, M. D., and S. M. Kreidenweis (2007), A single parameter representation of hygroscopic growth and cloud condensation nucleus activity, *Atmos. Chem. Phys.*, *7*, 1961–1971, doi:10.5194/acp-7-1961-2007.

Petters, M. D., S. M. Kreidenweis, A. J. Prenni, R. C. Sullivan, C. M. Carrico, K. A. Koehler, and P. J. Ziemann (2009a), Role of molecular size in cloud droplet activation, *Geophys. Res. Lett.*, *36*, L22801, doi:10.1029/2009GL040131.

Petters, M. D., H. Wex, C. M. Carrico, E. Hallbauer, A. Massling, G. R. McMeeking, L. Poulain, Z. Wu, S. M. Kreidenweis, and F. Stratmann (2009b), Towards closing the gap between hygroscopic growth and activation for secondary organic aerosol—Part 2: Theoretical approaches, *Atmos. Chem. Phys.*, *9*, 3999–4009, doi:10.5194/acp-9-3999-2009.

Poulain, L., Z. Wu, M. D. Petters, H. Wex, E. Hallbauer, B. Wehner, A. Massling, S. M. Kreidenweis, and F. Stratmann (2010), Towards closing the gap between hygroscopic growth and CCN activation for secondary organic aerosols—Part 3: Influence of the chemical composition on the hygroscopic properties and volatile fractions of aerosols, *Atmos. Chem. Phys.*, *10*, 3775–3785, doi:10.5194/acp-10-3775-2010.

Prenni, A. J., M. D. Petters, S. M. Kreidenweis, P. J. DeMott, and P. J. Ziemann (2007), Cloud droplet activation of secondary organic aerosol, *J. Geophys. Res.*, *112*, D10223, doi:10.1029/2006JD007963.

Roberts, G. C., and A. Nenes (2005), A continuous-flow streamwise thermal-gradient CCN chamber for atmospheric measurements, *Aerosol Sci. Technol.*, *39*, 206–221, doi:10.1080/027868290913988.

Roberts, G. C., D. A. Day, L. M. Russell, E. J. Dunlea, J. L. Jimenez, J. M. Tomlinson, D. R. Collins, Y. Shinozuka, and A. D. Clarke (2010), Characterization of particle cloud droplet activity and composition in the free troposphere and the boundary layer during INTEX-B, *Atmos. Chem. Phys.*, *10*, 6627–6644, doi:10.5194/acp-10-6627-2010.

Rosenørn, T., G. Kiss, and M. Bilde (2006), Cloud droplet activation of saccharides and levoglucosan particles, *Atmos. Environ.*, *40*, 1794–1802, doi:10.1016/j.atmosenv.2005.11.024.

Seinfeld, J. H., and S. N. Pandis (1998), *Atmospheric Chemistry and Physics: From Air Pollution to Climate Change*, Wiley Interscience, New York.

Shilling, J. E., et al. (2009), Loading-dependent elemental composition of α-pinene SOA particles, *Atmos. Chem. Phys.*, *9*, 771–782, doi:10.5194/acp-9-771-2009.

Svenningsson, B., and M. Bilde (2008), Relaxed step functions for evaluation of CCN counter data on size-separated aerosol particles, *J. Aerosol Sci.*, *39*, 592–608, doi:10.1016/j.jaerosci.2008.03.004.

Taira, M., and Y. Kanda (1990), Continuous generation system for low-concentration gaseous nitrous-acid, *Anal. Chem.*, *62*, 630–633, doi:10.1021/ac00205a018.

Taylor, J. R. (1997), *An Introduction to Error Analysis*, Univ. Sci. Books, Sausalito, Calif.

Tritscher, T., et al. (2011), Volatility and hygroscopicity of aging secondary organic aerosol in a smog chamber, *Atmos. Chem. Phys. Discuss.*, *11*, 7423–7467, doi:10.5194/acpd-11-7423-2011.

U. Baltensperger, J. Dommen, M. Gysel, T. Tritscher, and E. Weingartner, Laboratory of Atmospheric Chemistry, Paul Scherrer Institut, CH-5232 Villigen, Switzerland.

M. Bilde and M. Frosch, Department of Chemistry, University of Copenhagen, Universitetsparken 5, DK-2100 Copenhagen, Denmark. (mia@kiku.dk)

P. DeCarlo, Department of Civil, Architectural, and Environmental Engineering, Drexel University, Philadelphia, PA 19146, USA.

N. M. Donahue, Center for Atmospheric Particle Studies, Carnegie Mellon University, 5000 Forbes Ave., Pittsburgh, PA 15213, USA.

Z. Jurányi, School of Engineering, Institute of Aerosol and Sensor Technology, University of Applied Sciences Northwestern Switzerland, Klosterzelgstrasse 2, 5210 Windisch, Switzerland. (zsofia.juranyi@fhnw.ch)